International Research Journal of Engineering and Technology (IRJET) e-ISSN: 2395-0056
Volume: 13 Issue: 01 | Jan 2026 www.irjet.net p-ISSN: 2395-0072

Modeling the Vickers Hardness Response of HSS after Hardening–Tempering Heat Treatment Using Respon Surface Methodology

Afif Prasetya Nugraha Putra[1], Agus Suprihanto[1], Sri Nugroho[1]

[1] *Department of Mechanical Engineering, Faculty of Engineering, Diponegoro University, Semarang 50275, Indonesia*

Abstract - *This study examines the Vickers hardness response of SKH9 high-speed steel (HSS) after hardening–tempering heat treatment using Response Surface Methodology (RSM) with a two-factor interaction (2FI) model. Hardening temperature (850–950 °C) and tempering temperature (450–550 °C) were selected as the primary process variables, while Vickers hardness (HVN) was used as the response. All specimens were hardened for 15 minutes, quenched in water, and tempered for 60 minutes to ensure consistent processing conditions. The experimental results showed that the hardness varied from 448 to 505 HVN within the investigated parameter range, demonstrating a strong dependence on the applied heat treatment. Statistical analysis confirmed that the 2FI model is significant at the 95% confidence level, with tempering temperature identified as the dominant factor controlling hardness reduction. The response surface analysis indicated that high hardness is achieved by combining moderate-to-high hardening temperature with low tempering temperature, whereas lower hardness can be obtained by using high hardening temperature together with high tempering temperature. The developed response surface model provides an effective and practical framework for selecting hardening–tempering conditions to tailor the hardness of SKH9 HSS for specific application requirements.*

Key Words: High-Speed Steel (HSS); SKH9; Hardening–Tempering; Vickers Hardness; Response Surface Methodology

1. INTRODUCTION

High-Speed Steel (HSS) remains a principal engineering material for cutting tools and wear-critical components because it can sustain high hardness while retaining adequate toughness under severe thermo-mechanical loading [1], [2]. In practical manufacturing, the performance of HSS is not determined by chemical composition alone; it is strongly governed by the result of the applied hardening–tempering heat treatment, which establishes a hardened matrix together with a characteristic distribution of alloy carbides and a controlled fraction of retained austenite [3], [4], [5]. Consequently, parameter selection in the heat-treatment cycle is a decisive step in achieving the required hardness level and ensuring consistent product quality [6], [7].

Among the various property metrics used to qualify heat-treated HSS, hardness is one of the most widely adopted because it is closely associated with resistance to plastic deformation and edge retention in service. Vickers hardness (HV) is particularly suitable for laboratory-scale process development and model building due to its repeatability on small specimens and sensitivity to microstructural variations induced by thermal processing [8], [9], [10], [11]. However, optimizing hardness in HSS is not a simple monotonic "increase temperature to increase hardness" problem. During hardening (austenitizing), increasing temperature generally promotes dissolution of alloy carbides and enriches austenite with carbon and alloying elements, which can increase the hardness of martensite after quenching. Beyond an optimum window, excessive hardening temperature may produce adverse effects such as austenite grain coarsening and increased retained austenite, leading to reduced hardness or higher scatter [12], [13], [14], [15]. Tempering introduces additional complexity because it can either increase or decrease hardness depending on the competition between martensite decomposition and precipitation strengthening. Many HSS grades exhibit secondary hardening at appropriate tempering temperatures due to precipitation of fine alloy carbides; at higher temperatures and/or prolonged exposure, over-tempering and precipitate coarsening reduce strengthening and hardness [16], [17], [18], [19].

The current state of the art reflects three complementary streams of work. First, metallurgical investigations have established the mechanisms linking heat-treatment parameters to microstructure evolution particularly carbide precipitation behavior, retained austenite stability, and matrix transformations and have related these changes to mechanical properties, including hardness. These studies provide essential physical understanding of why hardness peaks can occur at intermediate conditions and why secondary hardening may be followed by softening at higher tempering temperatures. Second, industrial and handbook-based guidance offers recommended hardening and tempering practices for specific grades and applications, providing baseline parameter windows and emphasizing the need for strict thermal control to reach target hardness levels. Third, within the broader materials-processing literature, statistical design-of-experiments approaches especially Response Surface Methodology (RSM) implemented using structured designs are widely used to

build empirical process–property models, quantify main effects and interactions, and identify optimal regions with a limited number of experiments. RSM has proven effective for modeling hardness responses in heat-treatment-related studies because it captures curvature (quadratic behavior) and interaction terms that are typical of thermally driven metallurgical systems [20], [21], [22].

Despite this progress, a practical gap remains in many HSS heat-treatment studies and in industrial parameter development: hardness is often reported at discrete combinations of hardening and tempering conditions without providing a compact, statistically validated response-surface model that maps the parameter space to Vickers hardness within a clearly defined processing window [23], [24], [25], [26], [27]. This limitation is significant because the hardness response in HSS is frequently non-linear and interaction-sensitive; a beneficial change in hardening temperature may not yield improved hardness if the tempering temperature shifts the system toward over-tempering, while tempering conditions that promote secondary hardening may be ineffective if the preceding hardening stage does not establish the required solute and carbide state [28]. Without an explicit predictive surface, parameter selection tends to rely on iterative trials or generalized recommendations that may not fully match a given process window, equipment capability, or hardness target [29], [30], [31], [32].

Accordingly, this study focuses on the heat-treatment outcome post-process Vickers hardness of HSS and applies RSM to model and analyze the hardness response after hardening–tempering heat treatment. Hardening temperature and tempering temperature are treated as the primary independent variables within a controlled experimental domain, and a quadratic regression model is developed and assessed for adequacy. The resulting response surface is used to quantify the relative influence of each parameter and their interaction, and to identify the parameter region that maximizes Vickers hardness. By presenting hardness as a predictive surface rather than isolated data points, the work provides an evidence-based basis for parameter selection and supports practical heat-treatment tuning and process standardization for HSS applications.

2. MATERIAL AND METHODS

The material used in this study was High-Speed Steel (HSS) type SKH9, which is a tungsten–molybdenum–based tool steel widely used for cutting and wear-resistant applications due to its high hardness and good thermal stability after heat treatment [33]. All specimens were prepared from the same batch of SKH9 steel to minimize compositional variability. The samples were machined to identical dimensions suitable for hardness testing and were surface-ground prior to heat treatment to ensure uniform thermal exposure and consistent hardness measurements.

This study employed High-Speed Steel (HSS) type SKH9 as the experimental material. All specimens were prepared from the same material batch to minimize compositional variability. The samples were machined to identical dimensions suitable for hardness testing and surface-ground prior to heat treatment to ensure uniform thermal exposure and consistent indentation conditions during hardness measurements.

All specimens underwent a conventional hardening–tempering heat treatment sequence. During the hardening stage, the samples were heated in a controlled furnace to the designated temperature and held for 15 minutes to ensure sufficient austenitisation and thermal homogenization. Immediately after this period, the specimens were quenched in water, which was used as the quenching medium for all experimental runs in order to maintain consistent cooling severity. Tempering was subsequently carried out by reheating the quenched specimens to the specified tempering temperature and holding them for 60 minutes, followed by air cooling to room temperature. To isolate the effects of the selected variables on the hardness response, all parameters other than the hardening and tempering temperatures, holding times, heating rate, quenching medium and cooling conditions were kept constant.

To model the influence of heat treatment parameters on the hardness response of SKH9 HSS, a two-factor interaction (2FI) model based on Response Surface Methodology (RSM) was employed. Two independent variables were considered: hardening temperature (A) and tempering temperature (B). The experimental ranges were selected based on conventional heat treatment practices for SKH9: hardening temperature was varied from 850 to 950 °C, and tempering temperature from 450 to 550 °C. The experimental matrix consisted of a full combination of the selected factor levels, as summarized in Table 1. The response variable was defined as the Vickers hardness (HV) measured after the hardening–tempering cycle was complete.

Table -1: Experimental design and heat treatment parameters for SKH9 HSS

Run	Hardening Temperature (°C)	Hardening Holding Time (min)	Tempering Temperature (°C)	Tempering Holding Time (min)
1	850	15	450	60
2	900	15	450	60
3	950	15	450	60
4	850	15	500	60
5	900	15	500	60
6	950	15	500	60

7	850	15	550	60
8	900	15	550	60
9	950	15	550	60

Vickers hardness testing was performed after heat treatment. Prior to testing, the specimen surfaces were lightly polished to remove surface oxide layers and to ensure a smooth and flat indentation surface. Hardness measurements were conducted using a Vickers hardness tester under a constant test load and dwell time in accordance with standard testing procedures. For each experimental condition, multiple indentations were made at different locations on the specimen surface, and the average value was reported as the representative Vickers hardness to reduce the influence of local microstructural heterogeneity.

The experimental hardness data were analyzed using a two-factor interaction (2FI) regression model, which accounts for the main effects of hardening temperature and tempering temperature and their interaction, expressed in the general form [34]:

$$HV=\beta0+\beta1A+\beta2B+\beta12AB \quad (1)$$

Where HV is the Vickers hardness, A is the hardening temperature, B is the tempering temperature, and β\betaβ terms are the regression coefficients. Analysis of variance (ANOVA) was employed to evaluate the statistical significance of the main effects and interaction term, as well as the adequacy of the fitted model. The validated response surface was subsequently used to interpret the combined influence of hardening and tempering temperatures and to identify the parameter region associated with maximum hardness in SKH9 high-speed steel.

3. RESULT AND DISCUSSION

Table 2 summarizes the experimental matrix and the measured Vickers hardness (HVN) of SKH9 high-speed steel (HSS) after the hardening–tempering heat treatment. In all runs, the hardening stage was performed with a holding time of 15 minutes, followed by water quenching, and the tempering stage was carried out with a holding time of 60 minutes. The investigated variables were hardening temperature (A) and tempering temperature (B), while all other processing parameters were kept constant to isolate their effects on hardness.

The hardness values ranged from 448 to 505 HVN, confirming that the selected heat treatment parameters significantly influence the hardness outcome within the investigated domain. A clear trend observed from Table 2 is the strong effect of tempering temperature. Increasing tempering temperature generally reduced hardness, particularly at hardening temperatures of 900–950 °C. For example, at A = 900 °C, hardness decreased from 505 HVN at B = 450 °C to 483 HVN at B = 500 °C, and further to 448 HVN at B = 550 °C. This substantial reduction indicates that, within the tempering range of 450–550 °C, the hardness response is dominated by tempering-induced softening mechanisms, including martensite decomposition and over-tempering, which reduce the strengthening effect achieved after quenching.

Table -2: Experimental conditions and Vickers hardness results for SKH9 HSS

Run	Hardening Temperature, A (°C)	Tempering Temperature, B (°C)	Vickers Hardness (HVN)
1	850	450	485
2	900	450	505
3	950	450	503
4	850	500	468
5	900	500	483
6	950	500	474
7	850	550	495
8	900	550	448
9	950	550	450

The influence of hardening temperature was more condition-dependent and suggests the presence of an interaction with tempering temperature. At the lowest tempering temperature (B = 450 °C), increasing hardening temperature from 850 °C to 900 °C increased hardness from 485 to 505 HVN, while a further increase to 950 °C resulted in a slight decrease to 503 HVN. This behavior implies an optimum near 900 °C, where enhanced carbide dissolution and austenite enrichment can promote the formation of high-hardness martensite after water quenching. The slight reduction at 950 °C may be associated with adverse austenite conditions such as grain coarsening or increased retained austenite, which can reduce hardness despite higher austenitizing temperature.

At higher tempering temperatures, the benefits of increasing hardening temperature became less consistent. Notably, at B = 550 °C, the hardness at A = 850 °C reached 495 HVN, whereas hardness dropped markedly at A = 900–950 °C (448–450 HVN). This pattern indicates that the hardness response cannot be explained by the independent main effects alone; rather, the influence of hardening temperature depends on the tempering condition that follows. Such behavior is typical of heat treatment systems where the hardening stage establishes the as-quenched

microstructure (martensite/retained austenite and dissolved alloying content), while the tempering stage governs subsequent decomposition and precipitation processes. In practical terms, a hardening condition that is beneficial at lower tempering temperatures may not remain beneficial at higher tempering temperatures if the tempering step drives the microstructure toward over-tempering or otherwise reduces the as-quenched strengthening advantage.

To quantitatively capture this coupled behavior, Response Surface Methodology (RSM) was applied using a two-factor interaction (2FI) model, which considers the main effects of hardening temperature and tempering temperature as well as their interaction. The resulting response surface contour plot in Figure 1 serves as a processing map for the Vickers hardness of SKH9 HSS and clearly shows that the contour lines are not parallel to either axis, confirming the presence of interaction between the two thermal parameters. The contour map indicates that the highest hardness region (approximately 500–505 HVN) is achieved at a combination of moderate-to-high hardening temperatures (around 890–930 °C) and low tempering temperature (approximately 450 °C). This observation is consistent with the experimental results summarized in Table 2, where the maximum hardness of 505 HVN was obtained at A = 900 °C and B = 450 °C (Run 2).

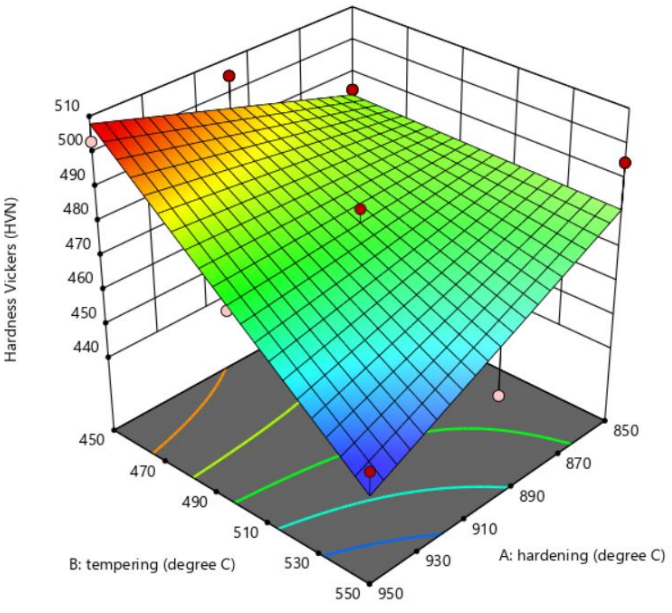

Fig -1: Respond surface on HSS SKH9 after heat treatment

Beyond identifying the optimum region, the response surface also provides practical insight into how different combinations of heat treatment parameters can be selected to tailor the hardness level. From the contour map, it can be observed that high hardness can be obtained by combining a high hardening temperature with a low tempering temperature, which promotes sufficient carbide dissolution during hardening while minimizing tempering-induced softening. Conversely, lower hardness levels can be deliberately achieved by using a high hardening temperature followed by a high tempering temperature, where the potential hardening benefit from elevated austenitizing is counteracted by enhanced martensite decomposition and over-tempering effects during tempering. This behavior highlights the flexibility of the hardening–tempering process in controlling the final hardness of SKH9 HSS through appropriate parameter combinations.

Previous studies have reported that increasing hardening temperature tends to increase attained hardness under consistent tempering conditions, while higher tempering temperatures lead to reduced hardness levels due to over-tempering effects on martensite and carbide evolution. For example, Mesquita et al. found that higher hardening temperatures result in higher hardness under the same tempering regime, and also discussed approaches to target lower hardness through adjustment of heat treatment parameters [35]. Liu et al. showed that tempering above the secondary hardening peak leads to a decline in hardness as carbide distribution evolves [18]. Barchukov et al. further discussed the effects of high-temperature tempering on hardness of high-speed steels, while Jovičević-Klug et al. highlighted the overall sensitivity of hardness to tempering temperature in high-speed steel variants [28].

Table -3: ANOVA for 2FI model on Hardness Vickers SKH9

Source	Sum of Squares	df	Mean Square	F-value	p-value
Model	2732.42	3	910.81	5.87	0.0429
A-hardening	73.50	1	73.50	0.4738	0.5219
B-tempering	1666.67	1	1666.67	10.74	0.0220
AB	992.25	1	992.25	6.40	0.0526
Residual	775.58	5	155.12		
Cor Total	3508.00	8			

The statistical validity of the 2FI model was evaluated using analysis of variance (ANOVA). The overall model was statistically significant at the 95% confidence level, with an F-value of 5.87 and a p-value of 0.0429, indicating that the selected factors and their interaction adequately explain the variation in hardness within the investigated domain. Among the individual terms, tempering temperature (B) exhibited a statistically significant effect (F = 10.74, p = 0.0220), confirming it as the dominant factor controlling hardness reduction. In contrast, the hardening temperature (A) main effect was not statistically significant (F = 0.47, p = 0.5219), suggesting that its influence on hardness is primarily

expressed through its interaction with tempering temperature rather than as an independent linear factor. The interaction term A×B yielded a marginal p-value ($p = 0.0526$), which, although slightly above the conventional 0.05 threshold, remains practically meaningful in the context of heat treatment processes where physical coupling between hardening and tempering stages is expected and is further supported by the observed non-parallel trends in Table 3 and the contour structure in Figure 1.

Overall, the combined experimental results, response surface contour analysis, and ANOVA demonstrate that joint control of hardening and tempering temperatures is essential for tailoring the hardness of SKH9 HSS. When maximum hardness is required, the response surface recommends a processing window characterized by high hardening temperature and low tempering temperature. Conversely, when a reduced hardness level is desired, the contour map indicates that high hardening temperature combined with high tempering temperature provides an effective route to achieve lower hardness through controlled over-tempering. These findings provide a clear, evidence-based framework for selecting heat treatment parameters based on the targeted hardness level.

4. CONCLUSIONS

This study investigated the Vickers hardness response of SKH9 high-speed steel (HSS) after hardening–tempering heat treatment using Response Surface Methodology (RSM) with a two-factor interaction (2FI) model. The experimental results demonstrated that the applied heat treatment parameters significantly influence the final hardness, with measured values ranging from 448 to 505 HVN within the investigated temperature domain. Statistical analysis confirmed that the developed 2FI model is significant at the 95% confidence level, indicating that the combined effects of hardening temperature, tempering temperature, and their interaction adequately describe the hardness variation of SKH9 HSS.

Among the investigated parameters, tempering temperature was identified as the dominant factor governing hardness reduction, whereas the effect of hardening temperature was primarily dependent on the selected tempering condition rather than acting as an independent linear factor. The response surface analysis showed that high hardness levels can be achieved by combining moderate-to-high hardening temperatures with low tempering temperature, with the maximum hardness of 505 HVN obtained at a hardening temperature of 900 °C and a tempering temperature of 450 °C. Conversely, lower hardness levels can be intentionally produced by employing high hardening temperature followed by high tempering temperature, where tempering-induced softening counteracts the hardening benefit from elevated austenitizing. Overall, the response surface model provides a practical and evidence-based framework for selecting hardening–tempering parameters to tailor the hardness of SKH9 HSS according to specific application requirements.

REFERENCES

[1] S. Shaojun, Z. Xianping, and S. Chengtong, “Heat-treatment and properties of high-speed steel cutting tools,” IOP Conf. Ser. Mater. Sci. Eng., vol. 423, no. 1, 2018, doi: 10.1088/1757-899X/423/1/012031.

[2] Y. Wang et al., “Advanced manufacturing of high-speed steels: A critical review of the process design, microstructural evolution, and engineering performance,” J. Mater. Res. Technol., vol. 24, pp. 8198–8240, May 2023, doi: 10.1016/j.jmrt.2023.04.269.

[3] Z. Wu et al., “Effect of microstructure on wear resistance during high temperature carburization heat treatment of heavy-duty gear steel,” Mater. Today Commun., vol. 40, p. 109486, Jun. 2024, doi: 10.1016/j.mtcomm.2024.109486.

[4] A. Saastamoinen, A. Kaijalainen, J. Heikkala, D. Porter, and P. Suikkanen, “The effect of tempering temperature on microstructure, mechanical properties and bendability of direct-quenched low-alloy strip steel,” Mater. Sci. Eng. A, vol. 730, pp. 284–294, 2018, doi: 10.1016/j.msea.2018.06.014.

[5] Z. Dai et al., “Fundamentals and application of solid-state phase transformations for advanced high strength steels containing metastable retained austenite,” Mater. Sci. Eng. R Reports, vol. 143, pp. 1–39, Jan. 2021, doi: 10.1016/j.mser.2020.100590.

[6] S. Omar and K. P. Plucknett, “The influence of DED process parameters and heat-treatment cycle on the microstructure and hardness of AISI D2 tool steel,” J. Manuf. Process., vol. 81, pp. 655–671, Sep. 2022, doi: 10.1016/j.jmapro.2022.06.069.

[7] M. Lindič, D. Klobčar, A. Nagode, N. Mole, B. Žužek, and T. Vuherer, “Heat treatment optimisation of 18 % Ni maraging steel produced by DED-ARC for enhancing mechanical properties,” J. Adv. Join. Process., vol. 11, p. 100312, 2025, doi: https://doi.org/10.1016/j.jajp.2025.100312.

[8] Q. Luo and M. Kitchen, “Microhardness, Indentation Size Effect and Real Hardness of Plastically Deformed Austenitic Hadfield Steel,” Materials (Basel)., vol. 16, no. 3, 2023, doi: 10.3390/ma16031117.

[9] A. D. Bagul and D. Kumar Dubey, “Effects on hardness by various heat treatments processes on HSS tool bit,” Mater. Today Proc., vol. 43, pp. 694–699, 2020,

doi: 10.1016/j.matpr.2020.12.619.

[10] K. Karolewska, M. Wirwicki, and B. Ligaj, "Evaluation of a Method for Determining Material Strength Based on Hardness Measurements: A Case Study of the Ti6Al4V Alloy.," Mater. (Basel, Switzerland), vol. 18, no. 16, Aug. 2025, doi: 10.3390/ma18163726.

[11] M. Fujita and K. Kuki, "An Evaluation of Mechanical Properties with the Hardness of Building Steel Structural Members for Reuse by NDT," Metals (Basel)., vol. 6, no. 10, 2016, doi: 10.3390/met6100247.

[12] M. Gebril, M. Aldlemy, and A. F.Khblan, "Effect of Austenization Temperatures and Times on Hardness, Microstructure and Corrosion Rate of High Carbon Steel," Springer, Des. Comput. Mod. Eng. Mater. Adv. Struct. Mater., vol. Volume 54, p. pp 421-428, Jul. 2014, doi: 10.1007/978-3-319-07383-5_30.

[13] R. Hossain, F. Pahlevani, and V. Sahajwalla, "Effect of small addition of Cr on stability of retained austenite in high carbon steel," Mater. Charact., vol. 125, Feb. 2017, doi: 10.1016/j.matchar.2017.02.001.

[14] S.-W. Young et al., "Effect of Alloying Elements on the High-Temperature Tempering of Fe-0.3N Martensite," Acta Mater., vol. 206, p. 116612, 2021, doi: https://doi.org/10.1016/j.actamat.2020.116612.

[15] W. Liu, X. Wang, F. Guo, and C. Shang, "Carbides Dissolution in 5Cr15MoV Martensitic Stainless Steel and New Insights into Its Effect on Microstructure and Hardness," Materials (Basel)., vol. 15, no. 24, 2022, doi: 10.3390/ma15248742.

[16] G. Krauss, "Tempering of Lath Martensite in Low and Medium Carbon Steels: Assessment and Challenges," steel Res. Int., vol. 88, p. 1700038, May 2017, doi: 10.1002/srin.201700038.

[17] Y. Liu et al., "Evolution of Microstructures and Mechanical Properties with Tempering Temperature in a Novel Synergistic Precipitation Strengthening Ultra-High Strength Steel.," Mater. (Basel, Switzerland), vol. 17, no. 21, Oct. 2024, doi: 10.3390/ma17215314.

[18] B. Liu et al., "Effect of Tempering Conditions on Secondary Hardening of Carbides and Retained Austenite in Spray-Formed M42 High-Speed Steel," Materials (Basel)., vol. 12, p. 3714, Nov. 2019, doi: 10.3390/ma12223714.

[19] D. Delagnes, P. Lamesle, M.-H. Mathon, N. Mebarki, and L. Christophe, "Influence of silicon content on the precipitation of secondary carbides and fatigue properties of a 5%Cr tempered martensitic steel," Mater. Sci. Eng. A, vol. 394, pp. 435–444, Mar. 2005, doi: 10.1016/j.msea.2004.11.050.

[20] A. Megalingam, A. Ahmad, T. D. Alang, J. Alias, and N. Razak, "Application of Response Surface Methodology for Parameter Optimization of Aluminum 7075 Thixoforming Feedstock Billet Production," J. Mater. Eng. Perform., Nov. 2022, doi: 10.1007/s11665-022-07535-4.

[21] V. Prabakaran, R. Palani, P. Saran, and S. Jenef, "Study of the tribological performance of pre- and post-heat treatment of AISI D2 steel with AlCrN coating under wet conditions," Aust. J. Multi-Disciplinary Eng., vol. 19, no. 1, pp. 18–29, Dec. 2023, doi: 10.1080/14488388.2023.2193377.

[22] V. Yarasu, B. Podgornik, B. S. Batic, M. Sedlacek, Č. Donik, and F. Ruiz-Zepeda, "Microstructure and mechanical performance of AISI D2 tool steel after standard and modified deep cryogenic treatment," Materialia, vol. 41, p. 102433, 2025, doi: https://doi.org/10.1016/j.mtla.2025.102433.

[23] Y. Wang, X. Ren, Z. Hou, A. Jiang, J. Zhao, and Z. Liu, "Optimization of Heat Treatment Process and Strengthening–Toughening and Mechanism for H13 Steel," Metals (Basel)., vol. 15, no. 10, 2025, doi: 10.3390/met15101101.

[24] S. Mudda, A. Hegde, S. Sharma, B. M. Gurumurthy, M. Shettar, and M. C. Gowrishankar, "Effect of various heat treatment methods and optimization of their parameters on mechanical properties of AISI 4140 steel.," Sci. Rep., vol. 15, no. 1, p. 31854, Aug. 2025, doi: 10.1038/s41598-025-17299-1.

[25] P. Biswas, A. Kundu, D. Mondal, and P. Bardhan, "Effect of heat treatment on microstructure behavior and hardness of EN 8 steel," IOP Conf. Ser. Mater. Sci. Eng., vol. 377, Jul. 2018, doi: 10.1088/1757-899X/377/1/012065.

[26] T. Pasang, Z. Chen, M. Ramezani, T. Neitzert, and D. Au, "The Effect of Heat Treatment Atmosphere on Hardening of Surface Region of H13 Tool Steel," J. Mater. Sci. Chem. Eng., vol. 1, pp. 20–29, Nov. 2013, doi: 10.4236/msce.2013.16004.

[27] A. Fortini, E. Bertarelli, M. Cassola, and M. Merlin, "An Industrial-Scale Study of the Hardness and Microstructural Effects of Isothermal Heat Treatment Parameters on EN 100CrMo7 Bearing Steel," Appl. Sci., vol. 14, no. 2, 2024, doi: 10.3390/app14020737.

[28] A. U. Lavrentiev, D. A. Barchukov, A. U. Lavrentiev, E. F. Romanenko, and A. V Filonovich, "HIGH-

TEMPERATURE TEMPERING OF HIGH-SPEED STEELS WITH MINIMUM CONTENT OF RETAINED AUSTENITE," pp. 621–625, 2017.

[29] Y. Jiang and J. Mohammadpour Velni, "A Soft Robotic Gripper for Crop Harvesting: Prototyping, Imaging, and Model-Based Control," AgriEngineering, vol. 7, no. 11, 2025, doi: 10.3390/agriengineering7110378.

[30] B. Lu et al., "When Machine Learning Meets 2D Materials: A Review," Adv. Sci., vol. 11, no. 13, p. 2305277, Apr. 2024, doi: https://doi.org/10.1002/advs.202305277.

[31] M. Kulichenko et al., "Data Generation for Machine Learning Interatomic Potentials and Beyond," Chem. Rev., vol. 124, no. 24, pp. 13681–13714, Dec. 2024, doi: 10.1021/acs.chemrev.4c00572.

[32] A. K. Kausik, A. Bin Rashid, R. F. Baki, and M. M. Jannat Maktum, "Machine learning algorithms for manufacturing quality assurance: A systematic review of performance metrics and applications," Array, vol. 26, p. 100393, 2025, doi: https://doi.org/10.1016/j.array.2025.100393.

[33] Y. Zhang, C. L. Hu, Z. Zhao, A. P. Li, X. L. Xu, and W. B. Shi, "Low cycle fatigue behaviour of a Cr–Mo–V matrix-type high-speed steel used for cold forging," Mater. Des., vol. 44, pp. 612–621, 2013, doi: https://doi.org/10.1016/j.matdes.2012.08.052.

[34] Y. Zhang, J. Pan, and L. Shi, "Construction of 2fi-optimal row–column designs," J. Stat. Plan. Inference, vol. 234, p. 106192, 2025, doi: https://doi.org/10.1016/j.jspi.2024.106192.

[35] R. Mesquita, C. Barbosa, C. Gonçalves, and A. Slaviero, "Effect of hardening conditions on mechanical properties of high speed steels," Int. Heat Treat. Surf. Eng., vol. 5, pp. 36–40, Mar. 2011, doi: 10.1179/174951411X12956208225221.